Physisorbed Rare-Gas Monolayers: Evidence for Domain-Wall Tilting

B. Grimm,* H. Hövel, M. Pollmann, and B. Reihl
University of Dortmund, Experimentelle Physik I, D-44221 Dortmund, Germany
(Received 26 January 1999)

We have studied the structure of Xe adsorbed on a highly oriented pyrolytic graphite surface in the submonolayer regime using scanning tunneling microscopy (STM) at $T = 5$ K. The Xe adlayer forms hexagonal domains in a honeycomblike superstructure. We observe domain walls tilted by roughly 12° with respect to the atomic rows of the Xe layer, which explains the previously found rotation of the diffraction pattern of about 0.5° relative to the ideal $(\sqrt{3} \times \sqrt{3})R30°$ layer. The STM signal exhibits a voltage-dependent contrast between Xe domains and domain walls, which can be understood by the different adsorption sites and the band structure of the Xe adlayer.

PACS numbers: 68.35.Bs, 61.16.Ch, 64.70.Rh, 73.20.At

Rare gases have a long tradition in serving as model systems in solid state physics as well as in surface science due to their spherical symmetry and simple electronic structure. Insight into the thermodynamics of phase transitions and general principles of two-dimensional (2D) ordering together with the formation of incommensurate adsorbate layers are obtained from the study of monolayers of rare gases on graphite. These systems provide ideal testing grounds for 2D adsorbate phases and phase transitions [1], as they exhibit a large variety of different phases originating from the fact that the lateral interaction of the rare gas atoms is of the same order of magnitude as the corrugation of the graphite surface potential [2]. The system "Xe on graphite" has been extensively studied by various experimental techniques such as low-energy electron diffraction [3,4], x-ray diffraction [5], transmission high-energy electron diffraction [6], and helium atom diffraction [7]. A wealth of theoretical work has been carried out on rare gases on graphite [8–13], and on the system Xe on graphite [14], in particular. Hence, the phase diagram of Xe on graphite is well known [6] along with many details in the monolayer-coverage regime [5].

Hong *et al.* [5] found a commensurate $(\sqrt{3} \times \sqrt{3})R30°$ Xe phase for the monolayer coverage at temperatures below $T = 60$ K, which was confirmed by other studies [5,6]. As the $(\sqrt{3} \times \sqrt{3})R30°$ lattice constant is about 3% smaller than the Xe bulk lattice constant, Xe forms an incommensurate phase in the submonolayer regime, because compressive strain is needed for the formation of the commensurate phase. This incommensurate phase exhibits a domain structure of commensurate domains separated by incommensurate domain-wall regions, which may either form a linear or honeycomblike array [1]. For the monolayer coverage of Xe on graphite, Hong *et al.* [5] observed the honeycomblike structure at temperatures between $T = 70–80$ K. Joos *et al.* [14] theoretically predicted an energetic preference for the hexagonal domain-wall structure in the submonolayer-coverage regime of Xe with domain sizes of about 10 nm.

In certain parts of the phase diagram, the incommensurate Xe adlayer is slightly rotated [5,6] with respect to the symmetry axes of the graphite substrate in agreement with the theory of Novaco and McTague [8]. These rotated incommensurate phases form a new class of structures, originating from the minimization of the strain energy by rotating the Xe overlayer. The structure of these rotated incommensurate phases was modeled by tilting the domain walls [9,10,12,13]. Although rotated incommensurate phases have been measured in diffraction experiments for different rare gas systems [5,6,15], a tilting of the domain walls has never been identified. Satellite Bragg peaks originating from the honeycomblike domain-wall structure could be observed only for nonrotated incommensurate phases due to intensity reasons [5].

The advent of scanning tunneling microscopy (STM) and its application to low-temperature surface-science systems has opened the possibility of real-space studies down to the atomic scale. The results presented in this Letter are to our knowledge the first STM study of the system Xe on graphite. For the submonolayer coverage, a tilting of the domain walls with respect to the symmetry axes of the Xe adlayer could directly be imaged.

The experiments were performed in a two-chamber surface-science facility, which has been described previously [16]. It consists of a preparation chamber equipped with a high-resolution hemispherical energy analyzer for ultraviolet photoelectron spectroscopy and an analysis chamber containing a low-temperature STM operating at $T = 5$ K [17]. The air-cleaved highly oriented pyrolytic graphite (HOPG) substrate was heated in UHV for one hour at $T = 870$ K prior to the experiments. We checked its cleanliness by ultraviolet photoemission.

The substrate was mounted on a manipulator and cooled to below $T = 50$ K by means of a liquid-helium flow cryostat. This manipulator allows cold sample transfer between the two chambers of the surface-science facility [16]. A submonolayer of Xe was dosed onto the sample by controlling the partial pressure with a leak valve. The Xe coverage was cross-checked by the Xe $5p$ photoemission signal during the adsorption process [18]. After adsorption, the sample was transferred into the STM, which was cooled to 5 K. The cooldown process of the sample takes

several minutes. The time scale for reaching thermal equilibrium at $T = 5$ K can be much longer, but the sample will be close to the low-temperature ground state after the cooldown process. However, differences in the adsorption temperature as the starting point of this process may influence the final structure of the Xe adlayer. The coverage got rechecked by photoemission after the STM experiments had been performed.

The STM topograph in Fig. 1(a) shows an atomically resolved surface area of 16×16 nm^2 with a nearest-neighbor distance inside a domain of 0.45 nm with an estimated error of approximately ± 0.05 nm. This distance is close to the expected $(\sqrt{3} \times \sqrt{3})R30°$ value of 0.426 nm for a Xe adlayer on a graphite surface and rules out the possibility that the atomic structure is due to the HOPG substrate. The STM image of Fig. 1(a) was recorded at a constant tunneling current of 0.1 nA and a gap voltage of $+3.2$ V with respect to the sample, as imaging was found to be stable in this voltage regime. At voltages below $+0.5$ V only the graphite substrate was imaged, which can be derived from the interatomic distances of 0.25 nm. The Xe atoms resolved in Fig. 1(a) form hexagonal patches about 15 atomic rows wide, separated by domain walls which appear in the STM signal as a smooth contrast several atomic rows in width. Xe atoms forming domain walls are slightly darker in the image than the surrounding Xe atoms in the domains. The origin of this contrast mechanism leading to an apparent height difference in the STM image of up to 0.03 nm will be discussed below.

The Xe domains in Fig. 1(a) are arranged in a hexagonal honeycomblike structure. This is in agreement with an incommensurate phase observed for a Xe coverage of 0.9 monolayers at temperatures $T < 60$ K [5]. It is also supported by theoretical predictions for a hexagonal domain-wall structure [14]. For a better illustration, two schematic models of the Xe overlayer are shown in Figs. 1(b) and 1(c). The Xe atoms are arranged in three possible domains denoted *A*, *B*, and *C*, each of which having an ideal $(\sqrt{3} \times \sqrt{3})R30°$ structure with respect to the graphite surface. In going from one domain to the neighboring one, the Xe rows are shifted by $a/2 = 0.12$ nm, where a denotes the lattice constant of graphite. In the STM image of Fig. 1(a), this shift can best be seen as a slight distortion of the Xe rows across the domain walls.

Contrary to the model of sharp superlight domain walls in terms of Ref. [1] we observe no vacant regions between two domains, which is consistent with the fact that the corrugation of the substrate-adsorption potential is relatively small, and, hence, completely uncovered regions would be energetically unfavorable [1]. Smooth domain walls with a width comparable to the domain sizes are theoretically predicted by Joos *et al.* [14]. For the Xe domains in Fig. 1(a), we measure approximately 5 nm as the distance between two opposite domain walls. We have studied several samples at different coverages well below one monolayer of Xe, exhibiting domain diameters between $L = 5$–10 nm with no systematic dependence on the Xe coverage. As the Xe-covered areas form close-packed islands larger than one micrometer in diameter as checked by STM, there should be no dependence on the Xe coverage. The crucial parameter in the evolution of the domains is the temperature during adsorption and insertion into the STM according to the procedure described above. For an estimation of this effect, we compare our domain sizes to data of Hong *et al.* [5] who

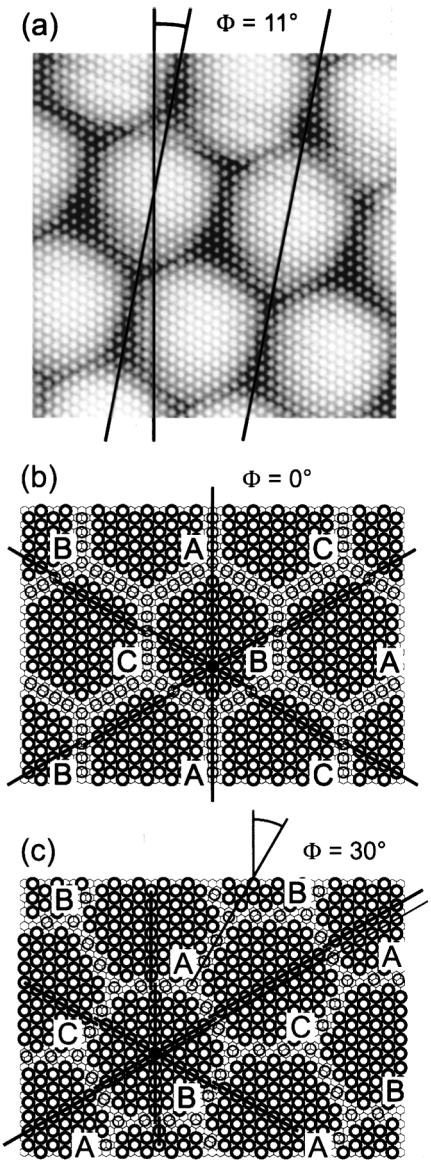

FIG. 1. (a) STM image of Xe on graphite showing atomically resolved hexagonal Xe domains arranged in a hexagonal honeycomblike structure. Image parameters: scan area, 16×16 nm^2; tip bias, 3.2 V; current, 0.1 nA. (b) and (c) Schematic models of the Xe overlayer structure with different orientations of the domain walls. Φ denotes the angle between the domain walls and the Xe atomic rows. Xe atoms are arranged in three possible domains (bold circles) denoted *A*, *B*, and *C*. Xe atoms forming domain walls are shown in thin circles. See text for a further discussion.

find a variation of the domain size by a factor of 2 for a temperature change of 14 K but for different Xe coverages. As our temperature uncertainty is about the same, we attribute the different domain sizes to variations in temperature during the Xe adsorption and sample-transfer processes.

We note that the symmetry axes of the honeycomb dislocation pattern in the STM image of Fig. 1(a) are not aligned with the symmetry axes of the Xe atoms as it is drawn in Fig. 1(b), but tilted by about $\Phi = 11°$. A systematic evaluation of our STM images of undistorted Xe areas as large as 50×50 nm^2 yield a tilt angle of $\Phi = 10°-15°$. It was found [5,6] for Xe submonolayer coverages that the diffraction pattern of the incommensurate phase in the low-temperature ground state of the Xe layer was rotated by a maximum angle of $\pm 0.6°$ [5] and $\pm 0.4°$ [6] with respect to the ideal $(\sqrt{3} \times \sqrt{3})R30°$ phase. As mentioned above, the theory of Novaco and McTague [8] had predicted a possible rotation of incommensurate adsorbate layers in order to minimize strain energy. Theoretical studies by Shiba [9] and Villain [10] also showed that an overall rotation of an adsorbate layer by a rotation angle φ can be related to a tilt of the domain walls by an angle Φ. The angle φ as measured in diffraction experiments is predicted [9,10] to be proportional to Φ and the inverse distance between domain walls.

For a discussion of the interdependence of Φ and φ, we show the situation for $\Phi = 0°$ [Fig. 1(b)] and $\Phi = 30°$ [Fig. 1(c)]. It is clear from simple symmetry considerations that the largest rotation φ of the overlayer structure occurs for a domain-wall tilt angle of $\Phi = 30°$ as depicted in Fig. 1(c). For $\Phi = 0°$, straight lines along the Xe atomic rows [cf. Fig. 1(b)] always cross just two of the three possible domains in an alternating manner. Hence, the overall displacement of the atomic rows and the rotation angle φ of the rows is zero. The same argument holds for $\Phi = n \times 60°$ with n integer. For $\Phi = 30°$, such lines [cf. Fig. 1(c)] cross all of the three different domains successively resulting in a finite rotation φ of the Xe atomic rows. We note that the domain structure has a threefold symmetry. With φ the monolayer rotation for domain walls tilted by an angle Φ, the monolayer is rotated by $(-\varphi)$ for a domain-wall tilt of $\Phi + 60°$. In summary, we suggest $\varphi \approx (a/L) \times \sin(3\Phi)$, which is consistent with Refs. [9,10] for $\Phi \ll 30°$. Though this picture is simplified, e.g., it neglects that the rotation of the diffraction pattern is an interference phenomenon, it gives a semiquantitative estimate. With our findings of $\Phi = 10°-15°$ and domain sizes $L = 5-10$ nm, we obtain a monolayer rotation φ of the order of 1°. This is in agreement with the rotation angles measured in Refs. [5,6]. Hence, we have identified the large tilting angle of the domain walls to be the origin of the small rotation angle observed in the diffraction studies [5,6].

Figure 2 shows a typical large-area STM image of 200×200 nm^2. The domain walls are clearly visible as a bright honeycomb pattern. The surface is locally contaminated by randomly distributed adsorbates appearing as bright spots. These adsorbates create distortions of the regular honeycomblike domain walls as has been discussed by Villain [11]. The presence of adsorbates creates a local preference for one certain domain leading to distortions of the wall structure.

The contrast inversion, in comparison with the measurement of Fig. 1(a), is due to the higher gap voltage applied (4.5 V). This increases the tip-sample separation, which was an advantage when taking large area overviews of the domain structure without atomic resolution. In Fig. 3, this voltage-dependent contrast of the domain-wall structure is shown in detail by STM line profiles across domain walls for different gap voltages. Tunneling conditions were found to be stable only at positive gap voltages (with respect to the sample) larger than 0.5 V. At low tunneling voltages, the domain walls appear to be imaged higher than the domains [cf. Fig. 3(a)], while the line profiles display atomic features. At higher voltages (above 2.0 V), this contrast is inverted [cf. Fig. 3(b)] along with an increased atomic corrugation. Around 4.5 V, there is a narrow resonancelike regime showing again domain walls higher than domains [cf. Fig. 3(c)] with an enhanced apparent height of the domain walls. In this voltage regime, the atomic corrugation disappears in the STM signal due to the increased tip-sample separation. Above 5.0 V, the domain-to-domain-wall contrast is inverted again [cf. Fig. 3(d)] and disappears above 6 V.

The gross effect enabling STM imaging of Xe on graphite is analogous to Xe on metal systems in which the Xe 6*s* resonance modifies the density of states at and above the Fermi level rendering the rare gas atoms visible

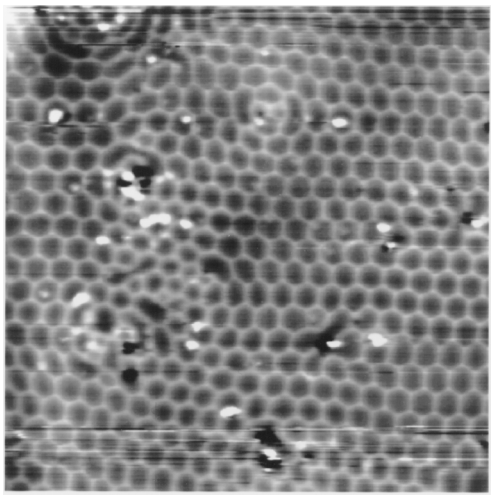

FIG. 2. STM image of Xe on graphite showing contamination-induced distortions in the hexagonal honeycomblike overlayer structure. Image parameters: scan area, 200×200 nm^2; tip bias, 4.5 V; current, 0.1 nA.

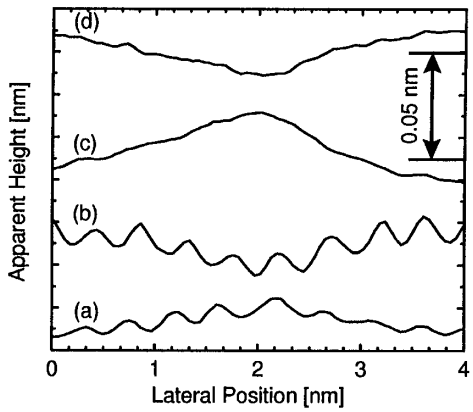

FIG. 3. STM line profiles across a Xe domain wall reflecting the voltage-dependent contrast between Xe domains and domain walls at different gap voltages: (*a*) $U = 1.1$ V; (*b*) $U = 3.7$ V; (*c*) $U = 4.5$ V; (*d*) $U = 5.3$ V. In (*a*) and (*b*), atomic features are clearly visible which disappear at higher voltages.

[19]. The dominant contribution to the tunneling current at low gap voltages is geometric in nature and originates from the different adsorption sites between domain walls and domains resulting in a buckling of the Xe layer, as has also been reported for other systems [20].

The contrast inversion at higher gap voltages is an electronic effect, which can be attributed to the lateral interaction of the Xe atoms within the adsorbate layer. This lateral interaction is strongly dependent on the interatomic distance as has been shown for the occupied states of the Xe monolayer [18,21]. It results in a broadening of the unoccupied Xe bands in the domain regions, which are then contributing to the tunneling current at lower gap voltages [22,23] as compared to the domain-wall regions, which consequently appear darker in the STM images. For a more detailed understanding, overall shifts in the band structure caused by the change in lattice parameter [24], different weighting factors for different wave vectors of the electronic states contributing to the tunneling current [22], and the possible influence of the tip have to be taken into account. The second inversion of the contrast between domains and domain walls around 4.5 V can be related to the unoccupied Xe $6p$ level located 4.3 V above the Fermi level in the monolayer coverage regime as has been shown for the system Xe on Au(110) by inverse photoemission [25]. A sharp peak in the energy distribution curve of the inverse-photoemission signal corresponds to a high density of states and causes a sudden contribution of these states to the STM signal of the domain walls, while the broadening of the energy bands in the case of the domains smears out and possibly shifts this contribution to higher energies.

In conclusion, we have performed a real-space study of the system Xe on HOPG using low-temperature STM. In the submonolayer regime, we have observed an incommensurate Xe adlayer with a honeycomblike pattern of domain walls. As a new experimental result, we have verified a tilt of the domain walls with respect to the Xe symmetry axes in accordance with theoretical predictions. The STM contrast between Xe domains and domain walls along with its voltage-dependent inversion could be attributed to the adsorption sites and the band structure of the Xe adlayer.

We thank G. Pike and F. Ströwer for their technical assistance with the experiments.

*Electronic address: grimm@physik.uni-dortmund.de; http://e1.physik.uni-dortmund.de

[1] R. J. Birgeneau and P. M. Horn, Science **232**, 329 (1986).
[2] W. J. Nuttall, K. P. Fahey, M. J. Young, B. Keimer, R. J. Birgeneau, and H. Suematsu, J. Phys. Condens. Matter **5**, 8159 (1993).
[3] J. J. Lander and J. Morrison, Surf. Sci. **6**, 1 (1967).
[4] J. Suzanne, J. P. Coulomb, and M. Bienfait, Surf. Sci. **40**, 414 (1973).
[5] H. Hong, C. J. Peters, A. Mak, R. J. Birgeneau, P. M. Horn, and H. Suematsu, Phys. Rev. B **40**, 4797 (1989).
[6] M. Hamichi, A. Q. D. Faisal, J. A. Venables, and R. Kariotis, Phys. Rev. B **39**, 415 (1989).
[7] G. Bracco, P. Cantini, A. Glachant, and R. Tatarek, Surf. Sci. **125**, L81 (1983).
[8] A. D. Novaco and J. P. McTague, Phys. Rev. Lett. **38**, 1286 (1977).
[9] H. Shiba, J. Phys. Soc. Jpn. **46**, 1852 (1979); H. Shiba, J. Phys. Soc. Jpn. **48**, 211 (1980).
[10] J. Villain, Phys. Rev. Lett. **41**, 36 (1978).
[11] J. Villain, J. Phys. (Paris), Lett. **41**, L267 (1980).
[12] V. L. Pokrovsky and A. L. Talapov, Phys. Rev. Lett. **42**, 65 (1979).
[13] N. D. Shrimpton and B. Joós, Phys. Rev. B **40**, 10 564 (1989).
[14] B. Joos, B. Bergersen, and M. L. Klein, Phys. Rev. B **28**, 7219 (1983).
[15] C. G. Shaw, S. C. Fain, Jr., and M. D. Chinn, Phys. Rev. Lett. **41**, 955 (1978); S. C. Fain, Jr., M. D. Chinn, and R. D. Diehl, Phys. Rev. B **21**, 4170 (1980); K. L. D'Amico, D. E. Moncton, E. D. Specht, R. J. Birgeneau, S. E. Nagler, and P. M. Horn, Phys. Rev. Lett. **53**, 2250 (1984).
[16] H. Hövel, T. Becker, D. Funnemann, B. Grimm, C. Quitmann, and B. Reihl, J. Electron Spectrosc. Relat. Phenom. **88–91**, 1015 (1998).
[17] T. Becker, H. Hövel, M. Tschudy, and B. Reihl, Appl. Phys. A **66**, 27 (1998).
[18] T. Mandel, M. Domke, and G. Kaindl, Surf. Sci. **197**, 81 (1988).
[19] D. M. Eigler, P. S. Weiss, E. K. Schweizer, and N. D. Lang, Phys. Rev. Lett. **66**, 1189 (1991).
[20] S. Horch, P. Zeppenfeld, and G. Comsa, Appl. Phys. A **60**, 147 (1995).
[21] K. Hermann, J. Noffke, and K. Horn, Phys. Rev. B **22**, 1022 (1980).
[22] V. A. Ukraintsev, Phys. Rev. B **53**, 11 176 (1996).
[23] J. Tersoff and D. R. Hamann, Phys. Rev. Lett. **50**, 1998 (1983).
[24] N. E. Christensen, Phys. Rev. B **20**, 3205 (1979).
[25] K. Horn, K. H. Frank, J. A. Wilder, and B. Reihl, Phys. Rev. Lett. **57**, 1064 (1986).